Diagnostic and Interventional Imaging (2016) **97**, 37—43

ORIGINAL ARTICLE / *ENT*

Warthin's tumor of parotid gland: Surgery or follow-up? Diagnostic value of a decisional algorithm with functional MRI

S. Espinoza*, A. Felter, D. Malinvaud, C. Badoual, G. Chatellier, N. Siauve, P. Halimi

Service de radiologie, hôpital Européen Georges-Pompidou, 20, rue Leblanc, 75015 Paris, France

KEYWORDS
Parotid gland tumor;
Functional MRI;
Warthin's tumor;
Decisional algorithm

Abstract
Purpose: Warthin's tumor is the second most frequent benign tumor of the parotid gland, with no risk of malignant evolution. That is why surgery should be avoided if the preoperative diagnosis is certain. The aim of the study was to assess the added value of a decisional algorithm for the preoperative diagnosis of Warthin's tumor.
Materials and methods: This retrospective IRB-approved study included 75 patients who underwent standardised MRI with conventional sequences (T1- and T2-weighted images, and T1 post-contrast sequences with fat saturation) and functional sequences: diffusion (*b*0, *b*1000) and perfusion MR. Two independent readers reviewed the images using the decisional algorithm. The conclusion of each reader was: the lesion is or is not a Warthin's tumor. The MRI conclusion was compared with histology or with cytology and follow-up. We calculated the Cohen's kappa coefficient between the two observers and the sensitivity and specificity of the algorithm-helped-reading for the diagnosis of Warthin's tumor.
Results: Seventy-five patients; histology ($n = 61$) or cytology and follow-up ($n = 14$) results revealed 20 Warthin's tumors and 55 other tumors. Using the algorithm, sensitivity and specificity were 80—96%, and 85—100%, respectively for readers 1 and 2. The Cohen's kappa coefficient between the two observers was 0.79 ($P < 0.05$) for the diagnosis of Warthin's tumor.
Conclusion: Our decisional algorithm helps the preoperative diagnosis of Warthin's tumor. The specificity of the technique is sufficient to avoid surgery if a parotid gland tumor presents all the MRI characteristics of a Warthin's tumor.

* Corresponding author.
E-mail address: sophie.espinoza@gmail.com (S. Espinoza).

http://dx.doi.org/10.1016/j.diii.2014.11.024

Warthin's tumor is the second most frequent benign tumor of the parotid gland (the first one is pleomorphic adenoma) [1]. This parotidian tumor occurs most often in smokers [2], in middle-aged and older men [3]. It is usually located at the inferior pole of the gland and multicentric occurrence is seen more often with Warthin's tumor than with any other salivary gland tumor [4]. Unlike pleomorphic adenomas, Warthin's tumor presents less than 1% risk of malignant evolution [5]. That is why surgery is not necessary when the preoperative diagnosis is certain and surgery should be avoided as often as possible because of the risk of facial nerve injury during surgery [6,7].

In this clinical context, when faced to a parotid gland tumor, MRI [8—12] and fine needle aspiration cytology (FNAC) are widely used before surgery [6,13]. FNAC is the most cost effective and minimally invasive way to determine the histological character of a parotid gland tumor. But, it is not always conclusive because the material may be insufficient. Furthermore, in case of Warthin's tumor, which contains inflammatory cells, FNAC can be responsible for an inflammatory flare with pain and volume increase of the lesion [14]. On the other hand, MRI accuracy for the diagnosis of Warthin's tumor has never been clearly reported, since in most studies, the aim was to distinguish the difference between malignant and benign lesions, pooling pleomorphic adenomas and Warthin's tumors [8—12]. As far as we know, there is only one study about Warthin's tumor and its MR diagnosis value [15], but the sensitivity and specificity of the technique are not reported in this study. That is why most surgeons are still going on surgical treatment for these benign tumors, despite of the risk of facial palsy [16]. Furthermore, to our knowledge, all the MR imaging studies tested the interest of anatomical sequences and/or functional sequences [8—12], but no study tested the interest of the whole examination, including all the available MR imaging data, it means: morphology, signal, diffusion with apparent diffusion coefficient (ADC) map, and dynamic contrast-enhanced MR imaging with time—intensity curve pattern, in order to establish the value of MR imaging for the diagnosis of Warthin's tumor. We have published a decisional algorithm for the interpretation of parotid gland tumor MR imaging, taking into account all the MRI data, including functional data [17].

The aim of the study was to assess the added value of our decisional algorithm for the preoperative diagnosis of Warthin's tumor.

Methods and materials

Patients

Between January 2006 and December 2012, our MR imaging database was retrospectively queried to identify all patients who underwent contrast-enhanced MR imaging of parotid gland ($n = 1039$). Patients with no parotid gland abnormality ($n = 901$; most often these MR examinations corresponded to MR follow-up after surgery), with inflammatory disease ($n = 6$) or with incomplete MR imaging ($n = 8$) where excluded. Mainly cystic lesions ($n = 3$) were excluded because it was not possible to place a region of interest in a tissular part, and then diffusion and perfusion sequences could not be analysed. Lesions less than 10 mm in diameter were excluded ($n = 2$) because they corresponded to

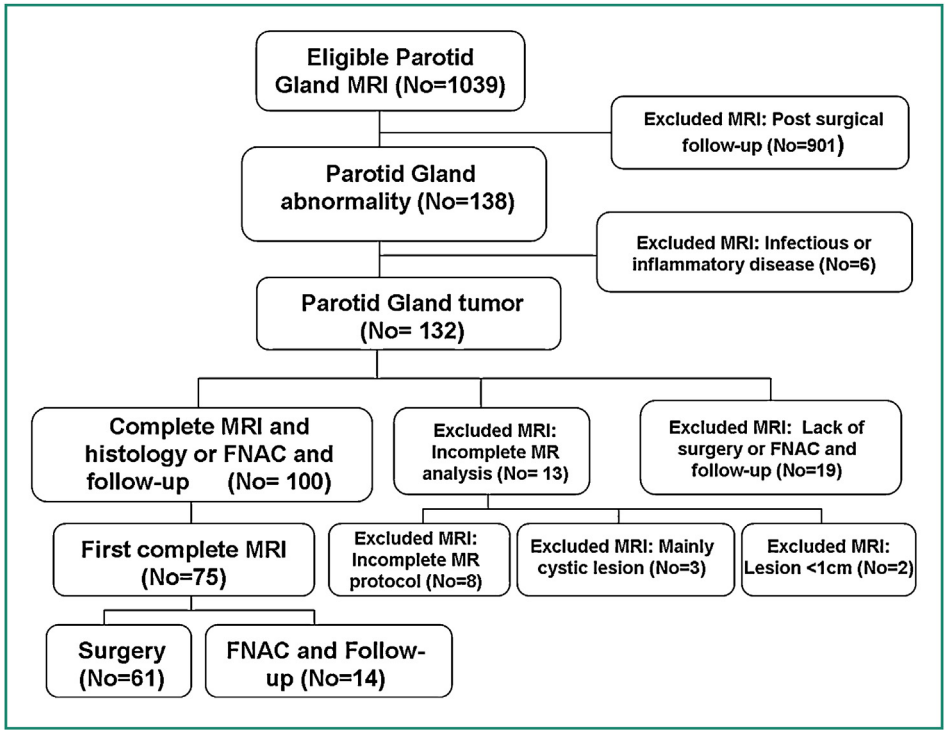

Figure 1. Flowchart shows patient population. Only the first complete MR imaging was selected. The final cohort included 75 patients. FNAC: fine needle cytology aspiration.

Table 1 Acquisition protocol.

Parameter	Sequence						
	Transverse T1-weighted FSE sequence	Transverse T2-weighted FR FSE sequence	Coronal T2-weighted FR FSE sequence	Transverse Diffusion weighted sequence	Perfusion Sequence	Transverse T1-weighted post Gadolinium with Fat saturation	Coronal T1-weighted post Gadolinium with Fat saturation
Repetition time (ms)	650	5350	3924	8000	7.4	488	519
Echo time (ms)	11.8	110	110	Min	2.16	Min full	Min full
Echo train length	2	16	16	—	—	4	3
Section thickness (mm)	4	4	4	5	4	4	4
Intersection gap (mm)	0.4	0.4	0.4	0	0	0.4	0.4
Field of view (mm)	180	240	180	280	280	170	190
Matrix	256 × 224	384 × 256	320 × 224	96 × 128	192 × 192	288 × 224	288 × 224
No of signals acquired	2	3	3	2	0.5	2	1
Bandwith (hHz)	31.25	41.67	31.25	250	25	31.25	19.23
Nb slices	30	33	22	30	50	28	21
Acquisition time (s)	148	134	173	64	180	243	125

intra parotid lymph nodes. Patients who did not undergo neither surgery nor fine needle aspiration cytology and at least 12 months clinical and MRI follow-up were excluded ($n = 19$). For patients who underwent multiple MR examinations, only the first complete MR imaging was selected ($n = 25$). The final cohort included 75 patients (Fig. 1). Our institutional ethics committee approved this retrospective study and waived the requirement to obtain informed consent.

MR Imaging technique

MRI was performed with a 1.5 T Signa HDX MR System (GE Medical Systems, Waukesha, WI, USA) using a head and neck phased array coil. The acquisition protocol (Table 1) included conventional sequences (transverse T1-weighted fast spin-echo, transverse and coronal T2-weighted FR fast spin-echo), and functional sequences (transverse diffusion weighted images with *b* values of 0 and 1000s/mm^2, and dynamic contrast-enhanced sequence in the transverse plane, after gadolinium chelate injection at a dose of 0.2 mL/kg via a power injector at a rate of 4 mL/s, followed by injection of 20 mL of normal saline to flush the tubing; images were obtained at a 3.6 s interval for 180 s). Finally, transverse and coronal T1-weighted fast spin-echo images with fat saturation were systematically acquired after injection of the gadolinium chelate.

MR image analysis

All exams were transferred to a workstation (ADW 4.2, GE Healthcare) and anonymized.

Two different radiologists with respectively 6 months and 8 years of experience in head and neck imaging, independently reviewed the images. Observers were blinded to MR imaging reports, clinical history, and results of pathologic examination.

Tumor side and size were recorded. Tumor margins were qualified: well defined tumor, lobulated tumor or irregular margins.

Signal analysis

On T1-weighted images, the signal intensity of the lesion was compared with the signal of the normal parotid gland parenchyma: low signal, iso-signal or high signal. We noted the homogeneous or heterogeneous character of the lesion. If high signal areas were present, we recorded the size of the high signal intensity zone: small spot or large area. On T2-weighted images, the signal of the lesion was compared with the signal of the normal parenchyma and with the signal of the cerebrospinal fluid on the posterior fossa: if the lesion signal was lower than normal gland parenchyma, the tumor signal was qualified as low signal; if the tumor signal was as high as the cerebrospinal fluid, it was qualified as high signal. Between these two categories, it was qualified as intermediary signal. The cystic component was defined as a tissue that showed high T1 signal intensity and/or did not enhance neither on perfusion sequence nor on late post-contrast images. By definition, the solid component showed enhancement after injection, on perfusion or late post-contrast images.

The DW images were analysed with the Functool Software (9.3.02e, GE Healthcare). On the apparent diffusion coefficient (ADC) map, 2 regions of interest (ROI) measuring

4 to 5 mm in diameter were placed: the first one in the solid component of the tumor and the second one in the normal contralateral gland. The ratio between the tumor ADC and the normal gland ADC was recorded.

The dynamic enhancement pattern was evaluated according to the Yabuuchi study [8] after positioning a 4 to 5 mm diameter region of interest in the solid part of the tumor: type A time—intensity curve corresponded to a gradual increase in the signal intensity, with a peak time longer than 120 s; in type B curve, time to peak was shorter than or equal to 120 s and the washout ratio [defined as follows: (SI max − SI 3 min)/(SI max − SI pre) × 100] was greater than or equal to 30%; in type C curve, time to peak was shorter than or equal to 120 s and the washout ratio was less than 30%. The only modification to the Yabuuchi protocol was a 3 min time sampling in our study compared with a 5 min time sampling in his study.

Lesion characterization

Tumors with irregular margins were considered as malignant tumors, and the algorithm was not used. For the other tumors, MR images were analysed according to our algorithm (Fig. 2). Both readers characterized the lesions as Warthin's tumors or other diagnoses (pleomorphic adenomas and malignant tumors were pooled). For both readers, and for each MR data set, the time necessary for the analysis was recorded.

Statistical analysis

We presented results according to the STARD statement recommendations [18].

The surgical pathologic findings (given by a pathologist with 15 years of experience in parotid gland tumors analysis) were used as the reference standard for the assessment of parotid tumors. For non-surgically-treated tumors, cytology (performed by a pathologist with a 23-year experience in parotid gland tumors cytology) associated with a one-year clinical and MRI follow-up were used as the reference standard.

For both readers, sensitivity, specificity, accuracy, positive and negative likelihood ratios, and positive and negative predictive values for the diagnosis of Warthin's tumor were calculated. The 95% confidence intervals were calculated according to the efficient-score method described by Newcombe [19]. To assess between radiologists agreement, we used the Cohen's kappa coefficient.

Results

Population

We included 75 patients (33 women, 42 men) with a mean age of 52.1 years. Tumors were located in the right parotid gland for 44 patients and in the left parotid gland for 31 patients.

Histological results were obtained for 61 patients; the 14 remaining patients underwent fine needle cytology aspiration and at least one-year clinical and MRI follow-up. Among the 75 tumors, 20 were Warthin's tumors, 39 were pleomorphic adenomas, 13 were malignant tumors and 3 were other benign tumors (1 oncocytoma, 1 basal cell adenoma, 1 myoepithelioma).

Table 2 Two by 2 diagnostic table for reader 1.

Reader 1	Histology		
	Warthin's tumor	Other tumor	Totals
Warthin's tumor	16	2	18
Other tumor	4	53	57
Totals	20	55	75

MRI results

The mean time required for analysis of one data set for readers 1 and 2 was 6.1 min and 5.7 min, respectively. The Cohen's kappa coefficient between the two observers was 0.79 ($P < 0.05$) for the diagnosis of Warthin's tumor.

The 2 by 2 diagnostic tables for each reader are shown in Tables 2 and 3. The accuracy of the technique for the diagnosis of Warthin's tumor was 92% and 96% respectively, for readers 1 and 2.

For the first reader, sensitivity and specificity of the technique for the diagnosis of Warthin's tumor were respectively: 80.0% (95% CI: 55.7%—93.3%) and 96.4% (95% CI: 86.4%—99.4%). There were 2 false positive results of Warthin's tumor: one low grade malignant tumor and one basal cell adenoma. Positive and negative likelihood ratios were respectively 22.0 (95% CI: 5.5—87.2) and 0.2 (95% CI: 0.1—0.5).

For the second reader, sensitivity and specificity of the technique for the diagnosis of Warhtin's tumor were respectively: 85.0% (95% CI: 61.1%—96.0%) and 100% (95% CI: 91.9%—100%). There was no false positive result. Positive and negative likelihood ratios were respectively not computable and 0.15 (95% CI: 0.05—0.43).

In our population, where the prevalence of Warthin's tumor was 26.7%, positive and negative predictive values were respectively 88.9% (95% CI: 63.9%—98.1%) and 93.0% (95% CI: 82.2%—97.7%) for reader 1 and 100% (95% CI: 77.1%—100%) and 94.8% (95% CI: 84.7%—98.7%) for reader 2.

Discussion

This study showed the value, for the diagnosis of Warthin's tumor, of our decisional algorithm, taking into account all

Table 3 Two by 2 diagnostic table for reader 2.

Reader 2	Histology		
	Warthin's tumor	Other tumor	Totals
Warthin's tumor	17	0	17
Other tumor	3	55	58
Totals	20	55	75

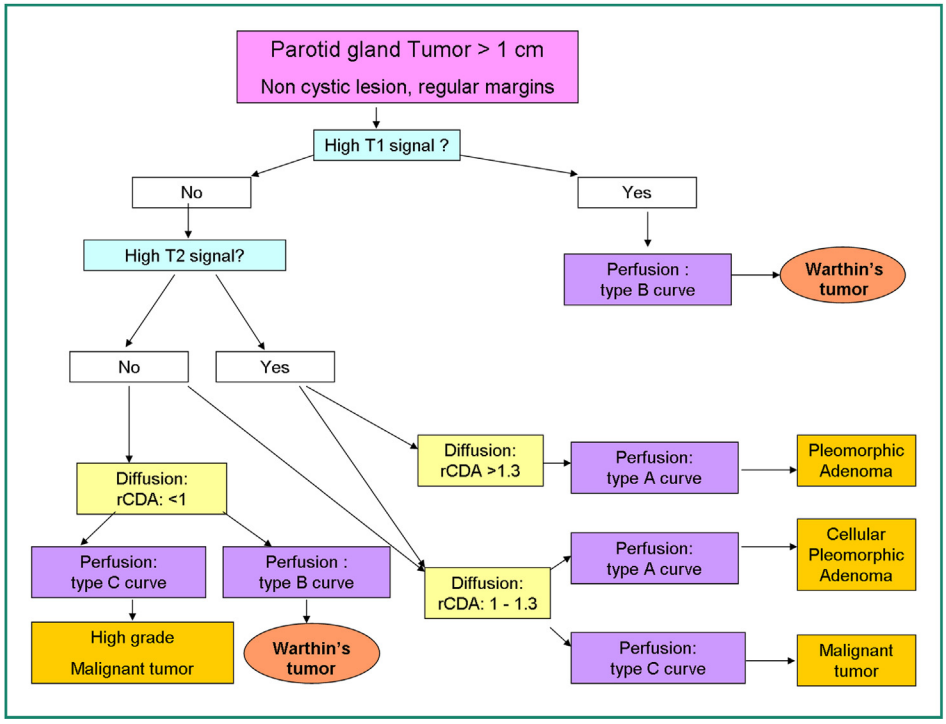

Figure 2. Algorithm used for MRI interpretation. Lesions less than 1 cm in diameter and mainly cystic lesions were excluded. Lesions with irregular margins were not classified with this algorithm.

the available MR data, including morphological, signal and functional data: the time of analysis for each data set is very reasonable; there is a good inter observers correlation, allowing to radiologists with few experience in head and neck imaging to achieve a very satisfactory specificity for the diagnosis of Warthin's tumor, very similar to the specificity of an experienced radiologist.

The very high specificity of this technique (96—100%) is very interesting because if the MR findings, according to our algorithm, are typical of a Warthin's tumor, the risk of error is very low, less than 4%. That means that the risk of avoiding a necessary surgery (for a malignant tumor or for a pleomorphic adenoma) is very low. This risk has to be compared with the risk of surgical complication: the most feared surgical complication is facial nerve injury with facial palsy. Most often, it is transient palsy, which is reported in 8—24% cases [20]. But it can also be permanent facial palsy, which is reported in 2—3% cases [21]. The high specificity of the technique for the preoperative diagnosis of Warthin's tumor means that there is a very low risk of false positive of diagnosis of Warthin's tumor. That is why we think that non-operative management of Warthin's tumors, when MRI findings are typical according to our algorithm, is a satisfactory option.

Reader 1 had 2 false positive results. The first one was a low grade malignant tumor, with no high T1 intensity zone, with an ADC ratio = 1.1. On the perfusion sequence, the washout ratio measured by reader 1 was 32%. For reader 2, the washout ratio was 29%. This difference was due to the ROI position. The second false positive result of reader 1 was a basal cell adenoma. It presented a large high T1 intensity zone. ADC ratio was 1.1. On the perfusion sequence, the washout ratio measured by reader 1 was 30%. For reader 2, the washout ratio was 26%. This difference was also due to the ROI position. Furthermore, unlike typical Warthin's tumors according to Yabuuchi study, for both lesions, time—intensity curves presented for both readers a low decreasing slope after the peak. These data emphasize the need to pay much attention to the ROI position, and to be very careful if the washout ratio is barely 30% on the time—intensity curve. We think that the slope after the peak is an important data: Warthin's tumors, in our study and in Yabuuchi study, presented after the peak a high negative slope which was not present in these two cases. Further studies should focus on this.

The sensitivity of this technique for the diagnosis of Warthin's tumor was found to be 80—85%. That means that both readers did not identify all the Warthin's tumors with this algorithm. These patients would have undergone non-useful surgery, but that is the most common management to date. As far as we know, this MR imaging sensitivity value for the diagnosis of Warthin's tumors is not reported in the literature since all studies, excepted Ikeda's study [15], have pooled pleomorphic adenomas and Warthin's tumors into a global benign tumor group. Ikeda et al. [15] did not pool Warthin's tumor and pleomorphic adenomas, but they only reported average ADC values and washout ratios, without giving us neither threshold values nor specificity values.

The accuracy of our technique was found to be 92—96%. This value is higher than the accuracy value of FNAC, which is reported to be 74—81% [22,23]. Hence, the risk of not performing a necessary surgical treatment after MRI is similar to the risk of error of FNAC [24].

Furthermore, in Warhtin's tumors, FNAC may induce parotiditis, without any relation to infection [14]. That is why, according to Suzuki et al. [14], we think that it may

be better to avoid systematic FNAC when faced to a lesion strongly suspected to be a Warthin's tumor after a complete MR imaging interpreted with our algorithm.

Our study had some limitations. Firstly, we had only 20 Warthin's tumors; but this prevalence is similar to what is reported in literature [25]. Secondly, only 7 Warthin's tumors were histologically proved, the 13 remaining only underwent FNAC and at least one-year MRI follow-up. But, the FNAC diagnosis of Warthin's tumor is reliable [24] and when coupled with appropriate clinical findings and one-year follow-up, the accuracy is very high [23,24]. Thirdly, we excluded tumors with no diffusion or perfusion workable data; it means that mainly cystic lesions and lesions less than 10 mm in diameter were all excluded because it was impossible to place a ROI on a tissular part. Warthin's tumors can present as cystic lesions. So our results are not useful for all parotid gland tumors but only for supra centimetric non-cystic lesions. In our study, these both categories of tumors represented 6.2% of the lesions ($n = 5/80$). Fourthly, we used the ADC ratio between the tumor and the contralateral normal gland, with our experimentally pre-established cut-off values. The ADC value of the normal gland can be modified by many factors, such as fat involution or acid consumption before the MR examination. But using the absolute ADC value, the results might be dependent on technical factors and might not be transferable to other institutions. Finally, the DCE sequence lasted for only 3 min, while in Yabuuchi study the cut-off value of 30% was defined after 5 min. But in our study the delay before the signal increase was only 20 s while in Yabuuchi study it was 60 s. It means that the difference was 80 s at the end of the sequence when the signal intensity decrease rate was very low, in both studies. We think that further studies should focus on the optimum delay for the calculation of the washout ratio, because some malignant lesions, with low signal intensity decrease, could present a washout ratio less than 30% 3 min after the contrast injection and more than 30% 5 min after the contrast injection. This may partially explain the very low number of false positive of Warthin's tumors in our study.

However, to our knowledge, this is the first report about the diagnostic value of a decisional algorithm, with functional MRI, for the diagnosis of Warthin's tumors.

Conclusion

In conclusion, our algorithm helps the diagnosis of Warhtin's tumor with MR imaging. The specificity of the technique is sufficient to avoid surgery when the parotid gland tumor presents all the MR characteristics of a Warthin's tumor.

Disclosure of interest

The authors declare that they have no conflicts of interest concerning this article.

References

[1] Guntinas-Lichius O, Klussmann JP, Wittekindt C, Stennert E. Parotidectomy for benign disease at university teching hospital: outcome of 963 operations. Laryngoscope 2006;116:534—40.
[2] Yu GY, Liu XB, Li ZL, Peng X. Smoking and the development of Warthin's tumour of the parotid gland. Br J Oral Maxillofac Surg 1998;36(3):183—5.
[3] Eveson JW, Cawson RA. Salivary gland tumours. A review of 2410 cases with particular reference to histological types, site, age and sex distribution. J Pathol 1985;146(1):51—8.
[4] Maiorano E, Lo Muzio L, Favia G, Piattelli A. Warthin's tumour: a study of 78 cases with emphasis on bilaterality, multifocality and association with other malignancies. Oral Oncol 2002;38(1):35—40.
[5] Som PM, Brandwein MS. Salivary glands: anatomy and pathology. In: Som PM, Curtin HD, editors. Head and neck imaging. 4th ed St. Louis, Mo: Mosby; 2005. p. 2003—133.
[6] Bradley PT, Paleri V, Homer JJ. Consensus statement by otolaryngologists on the diagnosis and management of benign parotid gland disease. Clin Otolaryngol 2012;37(4):300—4, http://dx.doi.org/10.1111/j.1749-4486.2012.02498.x.
[7] Yu GY, Ma DQ, Liu XB, Zhang MY, Zhang Q. Local excision of the parotid gland in the treatment of Warthin's tumour. Br J Oral Maxillofac Surg 1998;36(3):186—9.
[8] Yabuuchi H, Fukuya T, Tajima T, Hachitanda Y, Tomita K, Koga M. Salivary gland tumors: diagnostic value of gadolinium-enhanced dynamic MR imaging with histopathologic correlation. Radiology 2003;226(2):345—54.
[9] Eida S, Sumi M, Sakihama N, Takahashi H, Nakamura T. Apparent diffusion coefficient mapping of salivary gland tumors: prediction of the benignancy and malignancy. AJNR Am J Neuroradiol 2007;28(1):116—21.
[10] Thoeny HC. Imaging of salivary gland tumours. Cancer Imaging 2007;7:52—62 [Review].
[11] Yabuuchi H, et al. Parotid gland tumors: can addition of diffusion-weighted MR imaging to dynamic contrast-enhanced MR imaging improve diagnostic accuracy in characterization? Radiology 2008;249(3):909—16.
[12] Lechner Goyault J, Riehm S, Neuville A, Gentine A, Veillon F. Interest of diffusion-weighted and gadolinium-enhanced dynamic MR sequences for the diagnosis of parotid gland tumors. J Neuroradiol 2011;38(2:77-89):77—89.
[13] Raymond MR, Yoo JH, Heathcote JG, McLachlin CM, Lampe HB. Accuracy of fine-needle aspiration biopsy for Warthin's tumours. J Otolaryngol 2002;31(5):263—70.
[14] Suzuki K, Iwai H, Kaneko T, Sakaguchi M, Hoshino S, Inaba M. Induction of parotitis by fine-needle aspiration in parotid Warthin's tumor. Otolaryngol Head Neck Surg 2009;141(2):282—4.
[15] Ikeda M, et al. Warthin tumor of the parotid gland: diagnostic value of MR imaging with histopathologic correlation. AJNR Am J Neuroradiol 2004;25(7):1256—62.
[16] Thangarajah T, Reddy VM, Castellanos-Arango F, Panarese A. Current controversies in the management of Warthin tumour. Postgrad Med J 2009;85:3—8 [eview].
[17] Espinoza S, Halimi P. Interpretation pearls for MR imaging of parotid gland tumor. Eur Ann Otorhinolaryngol Head Neck Dis 2013;130(1):30—5.
[18] Bossuyt Patrick M, et al. For the STARD Group STARD towards complete and accurate reporting of studies of diagnostic accuracy: The STARD Initiative1radiol.2261021292. Radiology 2003;226:24—8.
[19] Newcombe RG. Two-sided confidence intervals for the single proportion: comparison of seven methods. Stat Med 1998;17:857—72.
[20] O'Brien CJ. Head Neck 2003 current management of benign parotid tumors-the role of limited superficial parotidectomy. Head Neck 2003;25(11):946—52.

[21] Dunn EJ, Kent T, Hines J, Cohn Jr I. Parotid neoplasms: a report of 250 cases and review of the literature. Ann Surg 1976;184(4):500—6.
[22] Ballo MS, Shin HJ, Sneige N. Sources of diagnostic error in the fine-needle aspiration diagnosis of Warthin's tumor and clues to a correct diagnosis. Diagn Cytopathol 1997;17:230—4.
[23] Parwani AV, Ali SZ. Diagnostic accuracy and pitfalls in fine-needle aspiration interpretation of Warthin tumor. Cancer 2003;99(3):166—71.
[24] Veder LL, Kerrebijn JD, Smedts FM, den Bakker MA. Diagnostic accuracy of fine-needle aspiration cytology in Warthin tumors. Head Neck 2010;32(12):1635—40.
[25] Wang YL, et al. Clinicopathologic study of 1176 salivary gland tumors in a Chinese population: experience of one cancer center 1997—2007. Acta Otolaryngol 2012;132(8): 879—86.